Validation of Coupled Simulation of Excavations in Saturated Clay: Camboinhas Case History

Christianne de Lyra Nogueira, D.Sc.[1]; Roberto Francisco de Azevedo, Ph.D.[2]; and Jorge Gabriel Zornberg, Ph.D., P.E., M.ASCE[3]

Abstract: This paper presents the results of an elastoplastic finite-element back analysis of an excavation made on a saturated soft organic clay deposit in Rio de Janeiro, Brazil. The excavation was conducted as part of an urbanization program, in which artificial islands were to be created in a swamp along the margins of the Camboinhas Lagoon. An extensive laboratory testing program was performed on undisturbed soil samples to characterize the stress-strain-strength behavior of the involved materials. Results from this laboratory testing program were used to calibrate a nonassociated elastoplastic constitutive model implemented in the ANLOG (Nonlinear Analysis of Geotechnical Problems) code. This code is based on the finite-element method and is capable of conducting fully coupled analyses by using a variety of constitutive models. Coupled analyses were performed to simulate the Camboinhas excavation, which was conducted under plane strain condition. Field measurements of both displacements and pore-water pressures obtained during the excavation are compared with the results of the numerical simulation. Analyses of the results show that monitored in situ and numerical results are in good agreement. **DOI: 10.1061/(ASCE)GM.1943-5622.0000077.** © *2011 American Society of Civil Engineers.*

CE Database subject headings: Excavation; Clays; Finite element method; Elastoplasticity; Measurement; Coupling; Case studies; Brazil.

Author keywords: Excavations; Finite-element methods; Elastoplastic; Field measurements; Coupled analysis; Case history.

Introduction

Excavations in soft soils are becoming more common to construct underground structures in densely populated urban areas. The movements in the adjacent soil mass induced by such excavations must be predicted, as measures may be undertaken, to prevent damage to nearby buildings and facilities.

The excavation-induced movements depend on initial ground conditions (i.e., stratigraphy, state of stress, and pore-water pressures), soils properties (i.e., stress-strain-strength behavior and hydraulic conductivity), and the sequence of excavation construction. Because analytical solutions that consider all of the aspects of this complex geotechnical problem are unavailable, numerical (e.g., finite element) analyses of excavation have been done since the late 1960s (e.g., Clough and Duncan 1969).

The numerical simulation of excavations involves determining the external forces that are equivalent to the unbalanced stresses along the excavation contour. Different approaches, involving a variety of interpolation procedures, have been adopted to obtain these external forces. Some of them were considered inappropriate (Christian and Wong 1973; Chandrasekaram and King 1974).

Mana (1978) presented a finite-element approach in which the external forces were obtained by numerically integrating the stress inside the removed elements adjacent to the contour of the excavation. Azevedo (1983) has shown that this procedure is meshing dependent; i.e., the exact magnitude of the external forces depends on the size of the removed element adjacent to the excavation contour. Consequently, a highly discretized mesh must be used near the excavation contour when adopting this procedure. Nonetheless, many authors have used this procedure (Osaimi 1977; Azevedo 1983; Zornberg 1989; Nogueira 1992; Azevedo et al. 1991, 2002).

Brown and Booker (1985), based on the work of Ghaboussi and Pecknold (1984), have shown that Mana's procedure does not guarantee equilibrium and that errors are propagated in each excavation stage. They proposed a new method to evaluate external forces by numerically integrating the stresses from body and surface forces in the remained domain, obeying static equilibrium equations. Borja et al. (1989) have shown that Brown and Booker's procedure provides a unique solution for any number of excavation stages.

Accuracy of the numerical simulation of excavations also depends on the capability of the constitutive models to represent the main features of soil behavior. Borja (1990) used a nonassociated elastoplastic constitutive model, based on critical state theory, to analyze a sequential excavation. Azevedo et al. (2001) simulated a tunnel in residual soil by using a nonassociated elastoplastic constitutive model. They showed that the results, in terms of monitored displacements using empirical approaches, from field instrumentation and those obtained by numerical simulations were in good agreement.

In the previously mentioned studies, the numerical simulations were conducted without considering the coupling between

[1]Associate Professor, Federal Univ. of Ouro Preto, Dept. of Mines Engineering, Campus Universitário, Ouro Preto, MG, Brazil, 35400-000 (corresponding author). E-mail: chris@em.ufop.br

[2]Titular Professor, Federal Univ. of Viçosa, Dept. of Civil Engineering, Campus Universitário, Viçosa, MG, Brazil, 36570-000. E-mail: razevedo@ufv.br

[3]Fluor Centennial Associate Professor, Univ. of Texas at Austin, Dept. of Civil Engineering, 1 University Station C1792, Austin, TX 78712-0280. E-mail: zornberg@mail.utexas.edu

Note. This manuscript was submitted on December 17, 2009; approved on July 1, 2010; published online on July 30, 2010. Discussion period open until November 1, 2011; separate discussions must be submitted for individual papers. This paper is part of the ***International Journal of Geomechanics***, Vol. 11, No. 3, June 1, 2011. ©ASCE, ISSN 1532-3641/2011/3-202–210/$25.00.

deformation and flow. However, such coupling must be considered when excavations are conducted in saturated soils of comparatively low hydraulic conductivity.

Yong et al. (1989) presented the coupled analysis (using finite elements) of a braced excavation conducted in Singapore. They used an associated elastic-perfectly plastic constitutive model that obeys the Mohr-Coulomb yield criterion. They showed the importance of considering a coupled analysis to estimate the progressive increase in lateral sheet pile movement and buildup of strut loads with time. Holt and Griffiths (1992) used the finite-element method to assess the transient behavior of an unsupported excavation. They used a nonassociated elastic-perfectly plastic soil model. Their results showed the relevance of excavation rate effect on excavation stability. Whittle et al. (1993) presented the coupled flow-deformation analysis of a deep braced excavation in Boston conducted in a clayey soil. They used the MIT-E3 elastoplastic constitutive model. Comparisons of numerical results and field measurements did not show good agreement in terms of lateral wall movements, lateral soil movements, settlements, and piezometric elevations. The authors attributed the discrepancies to the pore-water pressure boundary condition and to the construction sequence (excavation geometry and speed, floor slab installation, and dewatering) adopted in the numerical simulation.

This paper describes numerical analyses of an unsupported excavation made on a saturated soft organic clay deposit. Details of the material properties and excavation sequence are documented by Sandroni et al. (1984). Coupled flow and deformations analyses are conducted following the submerged multiple excavation construction stages by using an approach adapted from Brown and Booker's procedure and different constitutive models (Nogueira 1998).

The focus of this paper is on the comparisons between monitored in situ measurements of pore-water pressures, vertical and horizontal displacements, and results from the coupled finite-element simulations, using a constitutive model that has been having successful in soil behavior observed in laboratory tests (Azevedo and Farias 1987; Kim and Lade 1988; Lade and Kim 1988a, b; Laquini et al. 2007; Yang et al. 2008) and in analyses of some geotechnical constructions (Zornberg and Azevedo 1989; Azevedo et al. 1991; Azevedo and Melo 1996; Azevedo et al. 2002).

Project Description and Subsurface Conditions

The Camboinhas project was part of an urbanization development in which artificial islands were to be created in the swamp located along the margins of the Camboinhas Lagoon near Rio de Janeiro, Brazil (Sandroni et al. 1984).

The geotechnical profile at the site includes a 10.8-m thick organic clay layer underlain by a thick clayey sand layer (Fig. 1). The organic clay layer was fully saturated, as the water-table level was located 1.10 m over the top of the organic clay layer. Before initiating the project construction, the whole area was covered with a 1.7-m thick fill obtained by dredging clayey sands from the bottom of the lagoon.

Construction plans to create the artificial islands involved excavation of the fill and the upper part of the organic clay layer. To support the edges of excavation, crib walls ranging from 2 to 3 m high were constructed. Because these retaining structures needed to be constructed in dry conditions, the water in the trench had to be pumped before the construction of the crib walls. However, the excavation walls failed systematically during the lowering of the water table, preventing the crib walls construction.

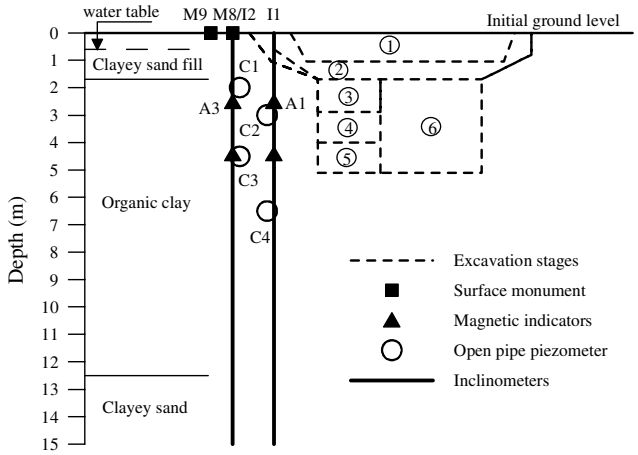

Fig. 1. Geotechnical profile, excavation geometry, and instrumentation

Because of these difficulties, a comprehensive investigation program was then undertaken, which included conducting an "in situ" program comprised by an experimental fill and excavation on the soft organic clay (Fig. 1). The fill was placed over the experimental site from December 1977 to January 1978 by using clayey sands dredged from the bottom of the lagoon. Settlements and pore pressures of the experimental fill were monitored. After six months, it was observed that primary consolidation of the soft clay layer caused by the fill surcharge was completed. Subsequently, the experimental excavation (approximately 5 m deep, 5 m wide, and 30 m long) was executed from July to August 1978. (Sandroni et al. 1984). The transverse cross section of the excavation was nonsymmetric to force failure to occur along the area where the instruments had been placed. The experimental excavation was long enough to assume plane strain equilibrium conditions in its middle longitudinal section (Silva 1979).

The excavation operations were executed in three phases. Phase 1 took six days and involved six excavation stages conducted under submerged conditions. The various excavations stages constructed at a rate of one stage per day are illustrated in Fig. 1. Phase 2 of the monitoring program consisted of a 45-day standing period. Phase 3 corresponds to lowering of the water table. Phase 3 was not simulated numerically, as the influence of lowering of water table is not considered in the finite-element formulation adopted in this study.

Soil Characteristics and Constitutive Models

An extensive laboratory testing program involving characterization tests, falling head permeability tests, drained and undrained conventional triaxial tests (CTC), and cubical triaxial tests was carried out to investigate the properties of the organic clay and clayey sand, the relevant soils for this study (Pinheiro 1980; Farias 1986).

The characterization test indicated the following properties index: porosity of approximately 37% and solids specific gravity of 2.64 for clayey sands and porosity of approximately 60%, plasticity index of 11%, and solids specific gravity of 2.025 for organic clay layer (Pinheiro 1980).

The saturated unit weight was 20.5 and 13.0 kN/m^3 for clayey sand and organic clay, respectively. The saturated hydraulic conductivity was 10^{-4} and 1.8×10^{-8} m/s for clayey sand and organic clay, respectively (Silva 1979; Pinheiro 1980).

The initial state of stress within the soil mass was defined by considering a geostatic condition with the water table initially

located 0.60 m below the fill surface. The at-rest earth pressure coefficient was estimated at 0.48 and 0.50 for clayey sand and organic clay, respectively, according to Noli (1980).

The effective frictional angle and cohesion were 30.9° and 14.1 kPa for clayey sand and 20.0° and 10.7 kPa for organic clay, respectively.

The elastoplastic analysis involved in this study was performed using the Lade-Kim's model (Kim and Lade 1988; Lade and Kim 1988a, b), which uses a single, isotropic yield surface, a nonassociated flow rule, and an isotropic work-hardening function. This constitutive model was adopted because of its capability to model several aspects of the stress-strain-strength characteristics of soils, such as the effects of the intermediate principal stress, shear-dilatancy, and stress-path dependency.

During the plastic flow, the strain increments are divided into elastic and plastic components. Elastic strain increments are obtained by using a nonlinear relation for the elastic modulus (E_{ur}) with the stress state as defined by Lade and Nelson (1987) and given by

$$E_{ur} = Mp_a\left[\frac{I_1}{p_a} + \left(6\frac{1+\nu}{1-2\nu}\right)\frac{I_{2D}}{p_a^2}\right]^{\lambda} \tag{1}$$

where M and λ = soil parameters obtained from linear regression of experimental test results; p_a = atmospheric pressure; ν = Poisson's coefficient; I_1 = first effective stress invariant; and I_{2D} = second invariant of the effective deviator stress.

The Poisson's ratio is assumed to be constant. For the organic clay layer, it was estimated at 0.22 as a function of the plastic index, as recommended by Lade (1979). The Poisson's ratio for the clayey sand layer was estimated at 0.40, according to Farias (1986).

To predict the plastic strain increments, the model requires defining the parameters for a yield surface, a hardening function, and a plastic potential function.

The yield criterion of the Lade-Kim model is given by

$$F(\sigma', W_p) = f(\sigma') - f(W_p) = 0 \tag{2}$$

where $f(\sigma')$ = yield function; and $f(W_p)$ = function of the plastic work (W_p).

The yield surface used in the elastoplastic model is convex in the principal effective stress space. It is represented by

$$f(\sigma') = \left(\psi_1\frac{I_1^3}{I_3} - \frac{I_1^2}{I_2}\right)\left(\frac{I_1}{p_a}\right)^h e^q \tag{3}$$

where I_1, I_2, I_3 = effective stress invariants; p_a = atmospheric pressure; h = yield surface function parameter; and q = function defined by

$$q = \left(\frac{\alpha S}{1-(1-\alpha)S}\right) \tag{4}$$

where α = yield surface function parameter; and S = stress level given by

$$S = \frac{(I_1^3/I_3 - 27)(I_1/p_a)^m}{\eta_1} \tag{5}$$

where m and η_1 = failure parameters obtained by linear regression of the peak stresses ($S = 1$).

To take into account the effect of tensile strength of the material, Lade and Kim (1995) introduced a nondimensional parameter a', which is defined as a function of the effective cohesion (c') and frictional angle (ϕ'), as follows:

$$a' = \frac{c'\cot g\phi'}{p_a} \tag{6}$$

Thus, a constant stress of magnitude $a'p_a$ is added to the normal effective stress before calculating the stress level [Eq. (5)].

In Eq. (3), ψ_1 = function of the failure parameter m given by

$$\psi_1 = 0.00155m^{-1.27} \tag{7}$$

As the yield surface represents a surface with equal plastic work, the parameter h of the yield surface can be obtained by applying Eq. (3) to a point A (at the hydrostatic axis) and to a point B (at the failure surface) of the same yield surface. Because the function q equals zero at point A, and this function equals unity at point B, the parameter h can be obtained as follows:

$$h = \log\left[\left(\psi_1\frac{I_{1B}^3}{I_{3B}} - \frac{I_{1B}^2}{I_{2B}}\right)e\Big/(27\psi_1+3)\right]\Big/\log(I_{1A}/I_{1B}) \tag{8}$$

where, I_{1B}, I_{2B}, and I_{3B} = effective stress invariants at peak condition (point B); and I_{1A} = first invariant of effective stress at hydrostatic condition (point A). The parameter h is calculated for each CTC test with different confining pressure. Then, the average value is adopted.

The plastic work function is represented by

$$f(W_p) = (27\psi_1+3)\left(\frac{W_p}{cp_a}\right)^{h/p} \tag{9}$$

where c and p = hardening parameters. These parameters are defined by linear regression of the plastic work values calculated from the hydrostatic compression (HC) test results (Nogueira 1998). According to the Lade-Kim model, during an HC test, the plastic work is given by

$$W_p = p_a c\left(\frac{I_1}{pa}\right)^p \tag{10}$$

The parameter α of the yield surface function is obtained by fitting experimental data to the following equation (Nogueira 1998):

$$q/S = \alpha + (1-\alpha)q \tag{11}$$

where S is given by the Eq. (5). The function q is obtained by considering the equality of Eqs. (3) and (8) according to the yield criterion on Eq. (2), as follows:

$$q = \ln\left\{\left[(27\psi_1-3)\left(\frac{W_p}{cp_a}\right)^{h/p}\right]\Big/\left[\left(\psi_1\frac{I_1^3}{I_3} - \frac{I_1^2}{I_2}\right)\left(\frac{I_1}{p_a}\right)^h\right]\right\} \tag{12}$$

The plastic work in Eq. (12) is given by

$$\begin{aligned} W_p &= \sum(\sigma_1' d\varepsilon_{1p} + 2\sigma_3' d\varepsilon_{3p}) \\ &= \sum[\sigma_1'(d\varepsilon_1 - d\varepsilon_{1e}) + 2\sigma_3'(d\varepsilon_3 - d\varepsilon_{3e})] \end{aligned} \tag{13}$$

where $d\varepsilon_1$ and $d\varepsilon_3$ = increments of axial and lateral strains occurring during the CTC tests; and $d\varepsilon_{1e}$ and $d\varepsilon_{3e}$ = elastic components of these increments. These elastic components can be calculated as follows:

$$d\varepsilon_{1e} = \frac{d(\sigma_1 - \sigma_3)}{E_{ur}} \tag{14}$$

$$d\varepsilon_{3e} = -\nu d\varepsilon_{1e} \tag{15}$$

where ν = Poisson's ratio; and E_{ur} = elastic modulus defined in Eq. (1).

The Lade-Kim model uses a nonassociative flow rule, in which the plastic potential function is given by

$$g(\sigma') = \left(\psi_1 \frac{I_1^3}{I_3} - \frac{I_1^2}{I_2} + \psi_2\right)\left(\frac{I_1}{p_a}\right)^{\mu} \tag{16}$$

where ψ_2 and μ = model parameters obtained by fitting experimental data to the following equation;

$$\xi_y = \frac{1}{\mu}\xi_x - \psi_2 \tag{17}$$

where

$$\xi_x = \frac{1}{1+\nu_p}\left[\frac{I_1^3}{I_2^2}(\sigma_1' + \sigma_3' + 2\nu_p\sigma_3') + \psi_1\frac{I_1^4}{I_3^2}(\sigma_1'\sigma_3' + \nu_p\sigma_3'^2)\right] - 3\psi_1\frac{I_1^3}{I_3} + 2\frac{I_1^2}{I_2} \tag{18}$$

$$\xi_y = \psi_1\frac{I_1^3}{I_3} + \frac{I_1^2}{I_2} \tag{19}$$

and

$$\nu_p = -\frac{d\varepsilon_{3p}}{d\varepsilon_{1p}} = -\frac{(d\varepsilon_3 - d\varepsilon_{3e})}{(d\varepsilon_1 - d\varepsilon_{1e})} \tag{20}$$

The approximation in Eq. (19) is obtained by linear regression considering all stress levels of all available CTC tests (Nogueira 1998).

The parameters used in elastoplastic analysis were obtained by calibrating the Lade-Kim model with the HC and CTC test results available in Pinheiro (1980) and Farias (1986). The calibration process consists of obtaining the elastic parameters by using unloading-reloading branches of the HC and/or CTC tests; by using the elastic parameters and the HC test results to determine the hardening parameters; and, with the parameters already calculated, by using the CTC test results to obtain the other parameters (Nogueira 1998). By using this methodology, elastoplastic parameters were defined for clayey sand ($M = 124.17$; $\lambda = 0.494$; $\nu = 0.40$; $\eta_1 = 59.6$; $m = 0.615$; $c = 0.00064$; $p = 1.52$; $\psi_2 = -3.010$; $\mu = 1.91$; $h = 0.789$; $\alpha = 0.691$; $a' = 0.23$) and organic clay ($M = 17.47$; $\lambda = 0.207$; $\nu = 0.22$; $\eta_1 = 17.9$; $m = 0.553$; $c = 0.00581$; $p = 1.52$; $\psi_2 = -3.081$; $\mu = 4.24$; $h = 0.854$; $\alpha = 0.407$; $a' = 0.29$).

These parameters were used to predict the stress-strain curves presented in Fig. 2. Theses curves were obtained by using an explicit integration schemes for integrating the constitutive equation. According to Sane et al. (2008), the calibration process should be done in two levels. Level 1 refers to the set of laboratory tests used to obtain the model parameters. In Level 2, the parameters obtained previously are used to predict laboratory tests that were not used in Level 1. In this paper, Level 2 was not performed because practical situations normally do not have laboratory test results beyond the indispensable ones.

Numerical Simulation of Camboinhas Excavation

Numerical simulations of the excavation sequence at the Camboinhas site were conducted using ANLOG (Nonlinear Analysis of Geotechnical Problems). This is a finite-element program developed for nonlinear analysis of geotechnical problems including the possibility of coupling analysis (Nogueira 1998). Quadratic quadrilateral isoparametric elements with eight nodes were used to approximate the displacements field, whereas linear quadrilateral superparametric elements with four nodes were used to approximate pore-water pressure field. In terms of pore-water pressure, the element is considered superparametic because the geometry is approximated by using quadratic interpolation functions, whereas the pore-water pressure field is approximated by using linear interpolation functions.

To model soil behavior, several constitutive relationships were implemented in the computer program ANLOG, including linear elastic, nonlinear elastic, and several associated and nonassociated elastoplastic models. As previously mentioned, the elastoplastic Lade-Kim model (Kim and Lade 1988; Lade and Kim 1988a, b) was used in the particular study described in this paper.

To account for the influence of the hydrostatic water pressure on the excavation numerical process, a new procedure was developed and implemented in the ANLOG code, based on Brown and Booker's concept (Nogueira et al. 2009). This new implementation and the coupled formulation were essential to numerically simulate the submerged Phases 1 and 2 of the Camboinhas excavation.

The initial state of stress within the soil mass was defined by considering a geostatic condition with the water table initially located 0.60 m below the fill surface. This water table remained

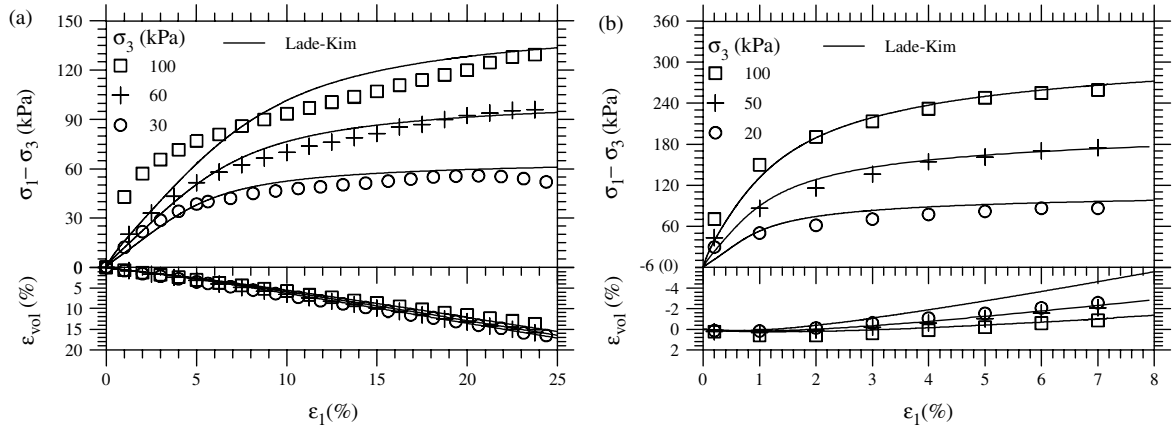

Fig. 2. CTC test data and Lade-Kim model results: (a) organic clay; (b) clayey sand

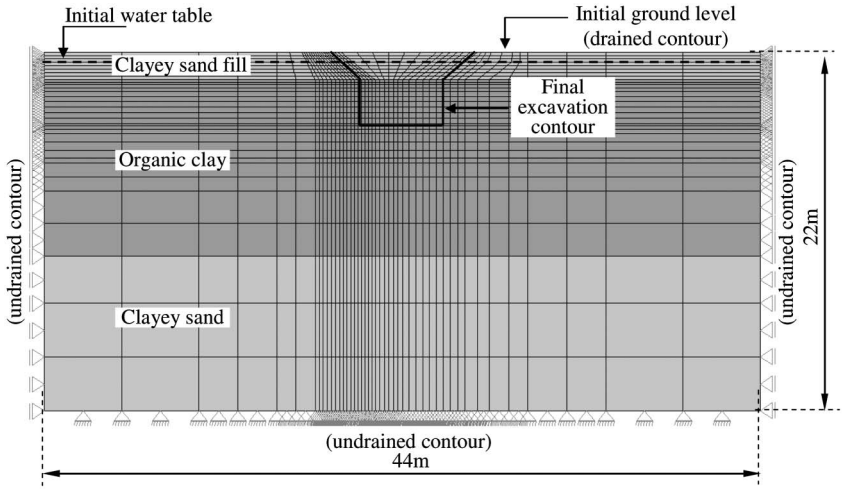

Fig. 3. Finite-element mesh used in simulation of Camboinhas excavation

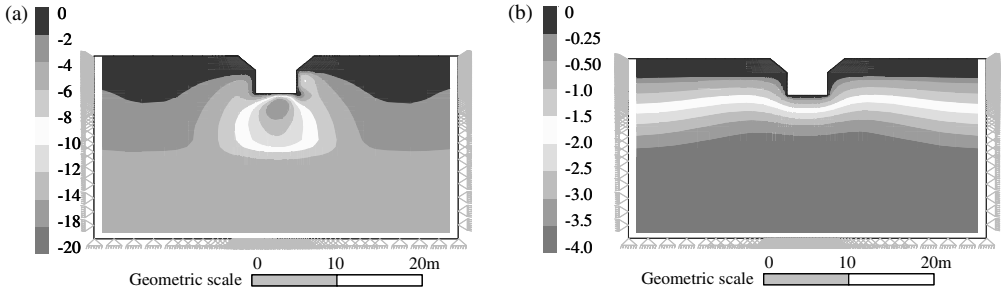

Fig. 4. Excess of pore-water pressure (kPa) obtained numerically: (a) end of Phase 1; (b) end of Phase 2

constant through Phases 1 and 2, and the organic clay and clayey sand were considered fully saturated.

Fig. 3 presents the mesh (1,440 elements and 4,475 nodal points) and boundary condition used to analyze the Camboinhas excavation. The pore-water pressure on the drained contour is assumed null, whereas the pore-water pressure on the undrained contour is unknown.

Fig. 4 shows the excess pore-water pressure field obtained numerically after simulating the excavation in six submerged stages, one stage per day (Phase 1) and after a 45-day standing period (Phase 2). Fig. 4(a) shows the excess pore-water pressure obtained immediately after completing Stage 6 (Phase 1) of excavation, and Fig. 4(b) shows the excess pore-water pressure field after the Phase 2 excavation. The magnitude of the generated excess of pore-water pressures at the bottom of excavation is approximately 80% of the effective weight of the soil removed by excavation [Fig. 4(a)]. This percentage is approximately 24% for the lateral of the excavation. In fact, according to Nogueira et al. (2009), an undrained response was expected for the organic clay because the order of magnitude of its hydraulic conductivity (10^{-3} m/day) is almost 1,000 times lower than that of the excavation rate (1 m/day). At the end of Phase 2, the excess pore-water pressures have dissipated almost completely.

Fig. 5 shows the variations of pore-water pressure with time during Phase 1, after each one of the six excavation stages, and at the end of Phase 2. This figure also compares the field monitoring results registered by piezometers C1, C2, C3, and C4 (Fig. 1) and the numerical results obtained in locations corresponding to these piezometers. It can be observed that the numerical results agree very well with the field data, particularly with results obtained from piezometers C1 and C2, which were located at position near surface. Piezometers C3 and C4 registered almost no variation of pore-water pressure, which is inconsistent with their field position near the excavation bottom, where the largest generation of excess pore-water pressures was expected. A possible reason for the results monitored using piezometers C3 and C4 is the slow time response of open tube piezometers.

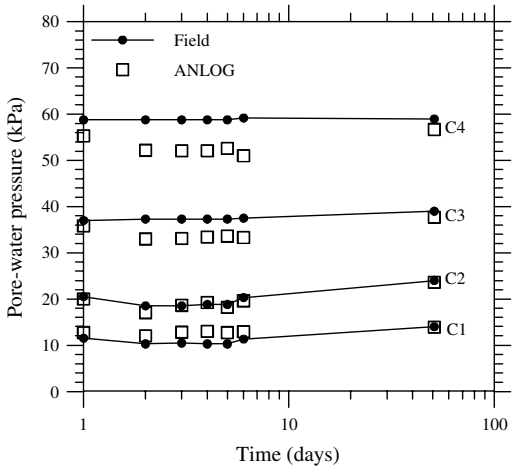

Fig. 5. Pore-water pressure measured from piezometers and obtained numerically

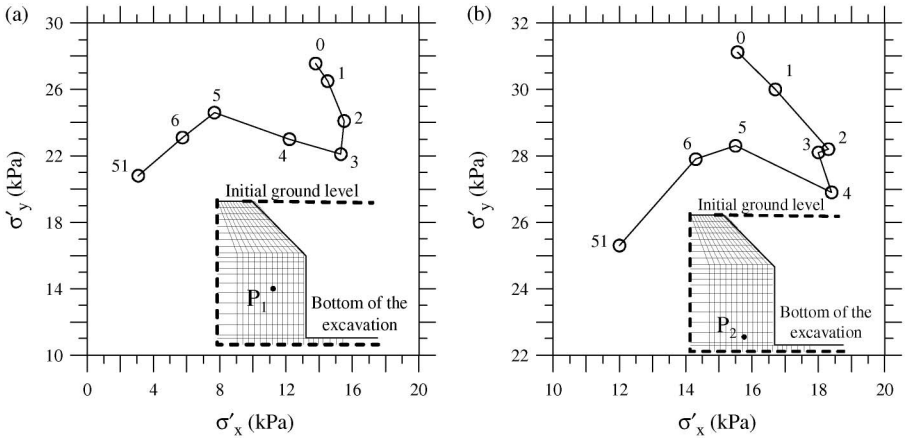

Fig. 6. Effective stress path obtained numerically: (a) location P_1; (b) location P_2

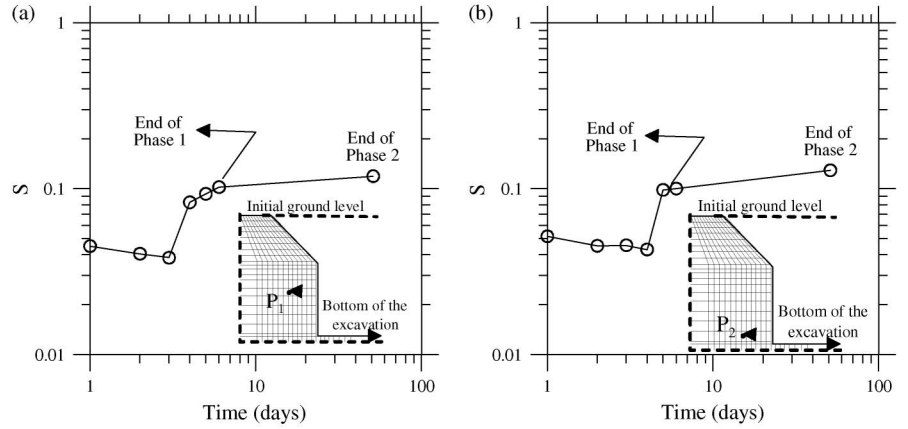

Fig. 7. Stress-level ratio (S) obtained numerically: (a) location P_1; (b) location P_2

Fig. 6 presents the effective stress paths obtained numerically in terms of the horizontal and vertical normal stresses at locations P_1 and P_2 during Phases 1 (from 0 to 6) and 2 (from 6 to 51). During Phase 1, it can be observed that vertical unloading (from 0 to 3) initially prevails in those points. From Stage 3 to 5, the horizontal unloading prevails over the vertical loading. An isotropic unloading can be observed from Stage 5 to 6. This pattern is in accordance with the sequence of the excavation stages. During Phase 2, isotropic unloading prevails in all points. According to the Lade-Kim model, elastic increment of strain predominates on vertical unloading stress path, producing upward vertical and outward horizontal movements. On the other hand, plastic increment of strain predominates during horizontal unloading stress path, producing downward vertical and inward horizontal movements.

Fig. 7 presents the stress ratio [Eq. (5)] at locations P_1 and P_2 during Phases 1 and 2. As it can be seen the stress level has increased during the excavation process, but it is far away from failure ($S = 1$). This is in accordance with the field observations that indicate no failure before lowering the water table (Phase 3).

Fig. 8 presents changes in surface vertical displacements with time as measured by surface monuments M8 and M9. The field data presented here refers only to the movement related to the

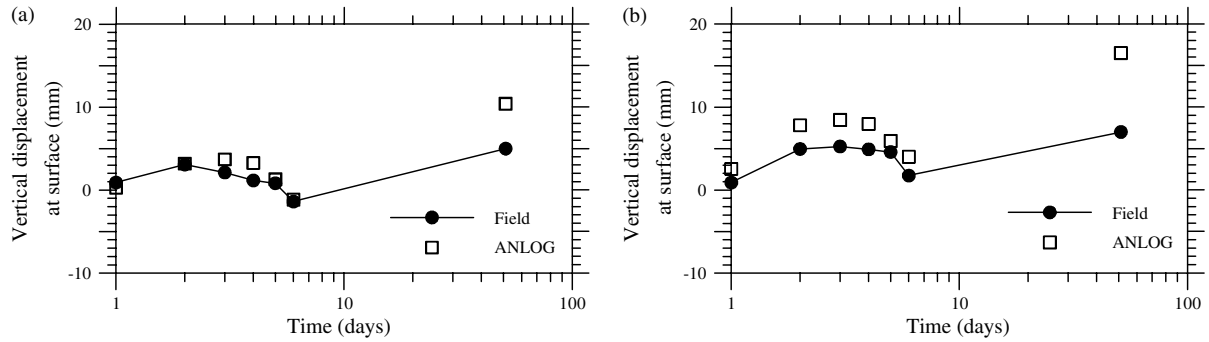

Fig. 8. Field-monitored vertical displacement at surface and obtained numerically: (a) location M9; (b) location M8

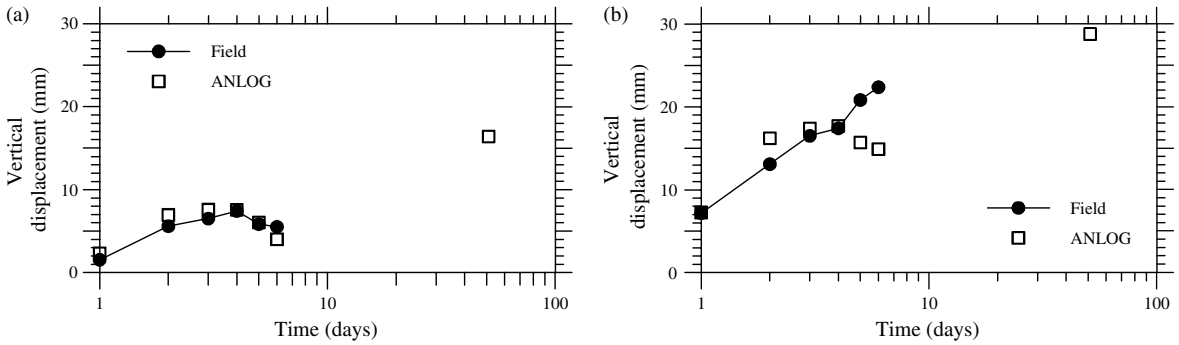

Fig. 9. Vertical displacements measured using magnetic indicator and obtained numerically: (a) location A3; (b) location A1

excavation process, i.e., the secondary compression of 1 cm/month (Sandroni et al. 1984), because the fill process was discounted since this parcel is not considered in the numerical analysis. The elastoplastic analysis leads to results that agree very well with the field monitoring data. Upward vertical movement is observed for the first three excavation stages, and a downward vertical movement is observed for the following excavation stages. The upward vertical movements agree with the unloading stress path followed during Phase 2.

Fig. 9 shows vertical displacements with time obtained by using field magnetic indicators measurements (A1 and A3) and results obtained numerically. Only Phase 1 results are presented because no field register was done during Phase 2. For initial excavation stages, both indicators measure upward movements. However, unlike magnetic indicator A3, indicator A1 shows continued upward vertical displacements even in the last excavation stages. This response is deemed unreasonable because downward vertical displacements are expected to predominate as the soil mass experiences a horizontal unloading. Therefore, magnetic indicator A3 was the one that worked properly, and for this instrument, the numerical solution obtained by the elastoplastic model compared very well with the corresponding field measurements.

Finally, Fig. 10 compares the horizontal displacement profiles measured by inclinometers I1 and I2 and the numerical results for the end of Stage 5 (Phase 1) excavation and for the end of Phase 2. Outward (positive) horizontal displacements dominate the response. These horizontal displacements tend to close the trench. The numerical results do not compare well with the field measurements except for inclinometer I2 [Fig. 10(a)], for which the magnitude of measured and predicted displacement are similar

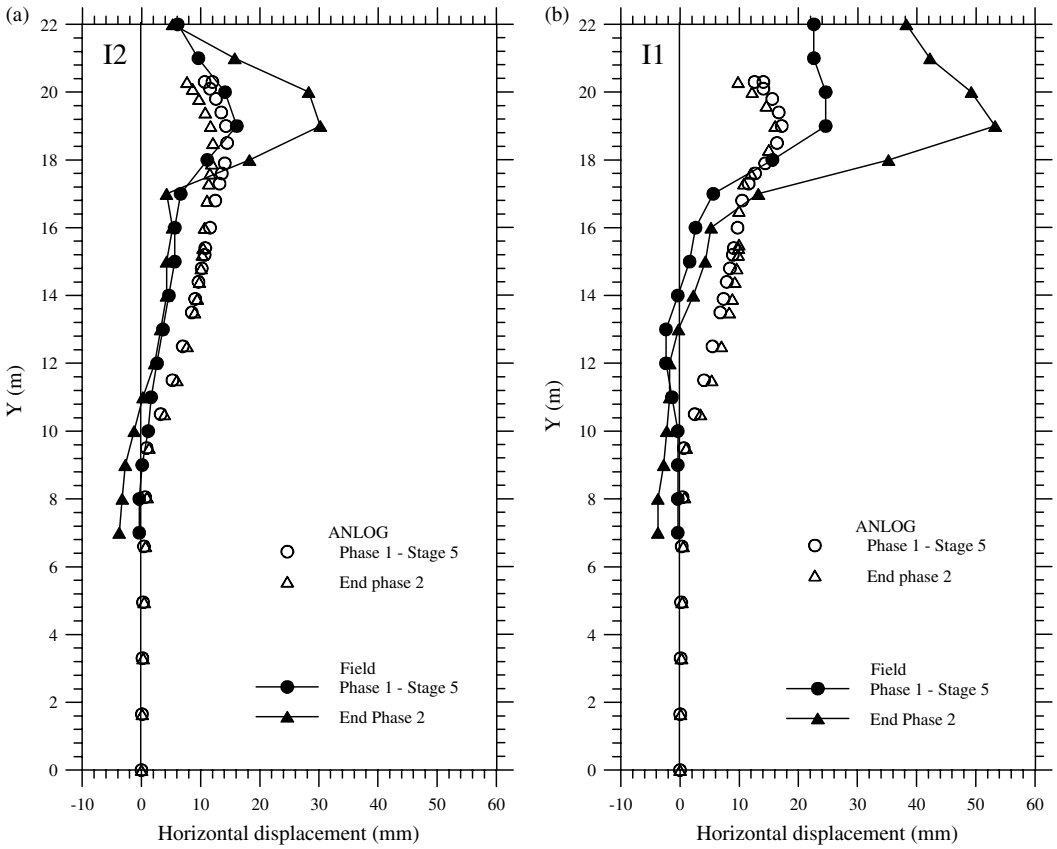

Fig. 10. Horizontal displacements at end of Stage 5 (Phase 1) and Phase 2 measured by inclinometers and obtained numerically: (a) location I2; (b) location I1

at the end of Stage 5 on Phase 1. An inward horizontal movement is expected to occur during Phase 2 because the soil has followed vertical and horizontal unloading effective stress path (Fig. 6). However, it is unreasonable that the horizontal movements continue to increase during the standing period, as indicated by the instrumentation. Moreover, the dissipation of small excess pore pressures (Fig. 4) are not expected to cause large horizontal movements as the ones measured in the field. Finally, Sandroni et al. (1984) mentioned that the inclinometers surveys were inconclusive. The upper part of inclinometer I1 was exposed during the earliest stage of the excavation process because of the erosion process on fill. Therefore, it is reasonable to attribute the observed differences to errors in the field measurements rather than in the numerical results.

Summary and Conclusions

Underground structures in crowded urban areas often demand excavation constructions. Many times, these structures are made below the water-table level and involve layers of soft soils. Naturally, movements in the adjacent ground must be evaluated to prevent damage to nearby buildings and facilities. The only way to calculate these movements, considering the importance of problems such as construction sequence and soil behavior, is by using numerical solutions. However, there is little information in technical literature presenting successful comparisons between numerical solutions and results obtained in the field by adequate instrumentation.

This paper presented the finite-element simulation of a well-instrumented unsupported excavation made in a soft clay deposit. The excavation was conducted below the water-table level. A coupled formulation using an elastoplastic constitutive model was adopted in the numerical simulation of the Camboinhas excavation. Comparisons between numerical and field measured results showed that

- Pore-water pressures and settlements variation with time from undrained to almost totally drained conditions were adequately simulated by the coupled numerical analyses.
- Vertical displacements at depth measured by a magnetic indicator during excavation (Phase 1) compared well with the numerical results. Unfortunately, during consolidation (Phase 2), the instrumentation results were not available for comparison.
- Horizontal movements registered by inclinometers did not match with those obtained numerically. However, the numerical results seem to be more reliable than the field results.

In conclusion, the use of a coupled flow and deformations analysis, together with an elastoplastic constitutive model properly calibrated using adequate laboratory tests, led to results ranging from undrained to drained conditions that fitted well with the consistent field-monitoring results.

Acknowledgments

The writers are grateful for the financial support received by the first writer from CAPES (Coordinating Agency for Advanced Training of High-Level Personnel—Brazil). They also acknowledge Prof. John P. White and Harriet K. Reis for their editorial review.

References

Azevedo, R. F. (1983). "Centrifugal and analytical modeling of excavation in sand." Ph.D. thesis, Univ. of Colorado at Boulder, Boulder, CO.

Azevedo, R. F., and Farias, M. M. (1987). "Elasto-plastic modeling of deformability and strength characteristics of a sand." *Proc., Int. Conference on Computational Plasticity: Models, Software and Applications*, Vol. 1, International Association on Computational Mechanics (IACM), Barcelona, Spain, 1527–1540.

Azevedo, R. F., and Melo, L. T. B. (1996). "O modelo elasto-plástico de Lade e Kim." *Revista Geotecnia, Sociedade Portuguesa de Geotecnia*, 75, 83–103 (in Portuguese).

Azevedo, R. F., Parreira, A. B., and Zornberg, J. G. (1991). "Elasto-plastic finite element analyses of a braced excavation and a tunnel." *Proc. of the 1st Int. Workshop on Applications of Computational Mechanics in Geotechnical Engineering*, Balkema, Rotterdam, Netherlands, 255–273.

Azevedo, R. F., Parreira, A. B., and Zornberg, J. G. (2002). "Numerical analysis of a tunnel in residual soil." *J. Geotech. Geoenviron. Eng.*, 128(3), 227–236.

Borja, R. I. (1990). "Analysis of incremental excavation based on critical state theory." *J. Geotech. Eng.*, 116(6), 964–985.

Borja, R. I., Lee, S. R., and Seed, R. B. (1989). "Numerical simulation of excavation in elastoplastic soils." *Int. J. Numer. Anal. Methods Geomech.*, 13, 231–249.

Brown, P. T., and Booker, J. R. (1985). "Finite element analysis of excavation." *Comput. Geotech.*, 1, 207–220.

Chandrasekaran, V. S., and King, G. J. (1974). "Simulation of excavations using finite elements." *J. Geotech. Engrg. Div.*, 100(9), 1086–1089.

Christian, J. T., and Wong, I. H. (1973). "Errors in simulating excavation in elastic media by finite elements." *Soils Found.*, 13(1), 1–10.

Clough, G. W., and Duncan, J. M. (1969). "Finite element analysis of Port Allen and Old River Locks." *Rep. No. TE69-3*, Office of Research Services, Univ. of California at Berkeley, Berkeley, CA.

Farias, M. M. (1986). "Construção e utilização de uma célula triaxial cúbica." M.Sc. thesis, Pontifícia Universidade Católica do Rio de Janeiro, Rio de Janeiro, Brazil (in Portuguese).

Ghaboussi, J., and Pecknold, D. A. (1984). "Incremental finite element analysis of geometrically altered structures." *Int. J. Numer. Methods Eng.*, 20, 2051–2064.

Holt, D. A., and Griffiths, D. V. (1992). "Transient analysis of excavations in soil." *Comput. Geotech.*, 13, 159–174.

Kim, M. K., and Lade, P. V. (1988). "Single hardening constitutive model for frictional materials—I. Plastic potential function." *Comput. Geotech.*, 5, 307–324.

Lade, P. V. (1979). "Stress-strain theory for normally consolidated clay." *Proc. 3rd Int. Conf. on Numerical Methods in Geomechanics*, W. Wittke, ed., Vol. 4, Balkema, Rotterdam, Netherlands, 1325–1337.

Lade, P. V., and Kim, M. K. (1988a). "Single hardening constitutive model for frictional materials—II. Yield criterion and plastic work contours." *Comput. Geotech.*, 6, 13–29.

Lade, P. V., and Kim, M. K. (1988b). "Single hardening constitutive model for frictional materials—III. Comparisons with experimental data." *Comput. Geotech.*, 6, 31–47.

Lade, P. V., and Kim, M. K. (1995). "Single hardening constitutive model for soil, rock and concrete." *Int. J. Solids Struct.*, 32(14), 1963–1978.

Lade, P. V., and Nelson, R. B. (1987). "Modeling the elastic behavior of granular matrial." *Int. J. Numer. Anal. Methods Geomech.*, 11, 521–542.

Laquini, J. P., Azevedo, R. F., and Reis, R. M. (2007). "Elasto-plastic modeling of saturated and non-saturated residual soil." *Electronic J. Geotech. Eng.*, 12, 1–10.

Mana, A. I. (1978). "Finite element analyses of deep excavation in soft clay." Ph.D. thesis, Stanford Univ., Stanford, CA.

Nogueira, C. L. (1992). "Análise de escavações com acoplamento de fluxo e deformações." M.Sc. thesis, Pontifícia Universidade Católica do Rio de Janeiro, Rio de Janeiro, Brazil (in Portuguese).

Nogueira, C. L. (1998). "Análise não-linear de escavações e aterros." D.Sc. thesis, Pontifícia Universidade Católica do Rio de Janeiro, Rio de Janeiro, Brazil (in Portuguese).

Nogueira, C. L., Azevedo, R. F., and Zornberg, J. G. (2009). "Coupled analyses of excavation in saturated soil." *Int. J. Geomech.*, 9(2), 73–81.

Noli, L. A. O. (1980). "Análise paramétrica linear elástica da escavação de camboinhas." M.Sc. thesis, Pontifícia Universidade Católica do Rio de Janeiro, Rio de Janeiro, Brazil (in Portuguese).

Osaimi, A. E. (1977). "Finite element analysis of the time dependent deformations and pore pressures in excavations and embankments." Ph.D. thesis, Stanford Univ., Stanford, CA.

Pinheiro, J. C. N. (1980). "Ensaios triaxiais em depósito mole turfoso na margem oeste da Lagoa de Itaipu, RJ." M.Sc. thesis, Pontificia Universidade Católica do Rio de Janeiro, Rio de Janeiro, Brazil (in Portuguese).

Sandroni, S. S., Silva, J. M., and Pinheiro, J. C. N. (1984). "Site investigations for retaining excavation in a soft peaty deposit." *Can. Geotech. J.*, 21, 36–59.

Sane, S. M., Desai, C. S., Jenson, J. W., Contractor, D. N., Carlson, A. E., and Clark, P. U. (2008). "Disturbed state constitutive modeling of two Pleistocene tills." *Quat. Sci. Rev.*, 27(3–4), 267–283.

Silva, J. M. J. (1979). "Instrumentação, acompanhamento e análise preliminar de escavação experimental no depósito orgânico à margem oeste da Lagoa de Itaipu, RJ." M.Sc. thesis, Pontificia Universidade Católica do Rio de Janeiro, Rio de Janeiro, Brazil (in Portuguese).

Whittle, J. A., Hashash, Y. M. A., and Whitman, R. V. (1993). "Analysis of deep excavation in Boston." *J. Geotech. Engrg. Div.*, 119(1), 69–90.

Yang, K.-H., Nogueira, C. L., and Zornberg, J. G. (2008). "Isotropic work softening model for frictional geomaterials: Development based on Lade and Kim soil constitutive model." *Proc., 29th Iberian Latin American Congress on Computational Methods in Engineering, CILAMCE 2008* (CD-ROM), Brazilian Association of Computational Methods in Engineering, Rio de Janeiro, Brazil, 1–17.

Yong, K. Y., Lee, F. H., Parnploy, U., and Lee, S. L. (1989). "Elastoplastic consolidation analysis for strutted excavation in clay." *Comput. Geotech.*, 8, 311–328.

Zornberg, J. G. (1989). "Análise por elementos finitos do comportamento de escavações utilizando um modelo elasto-plástico." M.Sc. thesis, Pontificia Universidade Católica do Rio de Janeiro, Rio de Janeiro, Brazil (in Portuguese).

Zornberg, J. G., and Azevedo, R. F. (1989). "Análise por elementos finitos da superfície de ruptura de escavações à céu aberto utilizando um modelo elasto-plástico não-associado." *Revista de Mecânica Computacional*, 7, 361–374 (in Portuguese).